Available online at www.sciencedirect.com
ScienceDirect
C. R. Mecanique 335 (2007) 253–260
COMPTES RENDUS MECANIQUE
http://france.elsevier.com/direct/CRAS2B/

Melting and solidification: processes and models/Flows in solidification

Secondary and oscillatory gravitational instabilities in canonical three-dimensional models of crystal growth from the melt. Part 1: Rayleigh–Bénard systems

Marcello Lappa [a,b,*]

[a] *MARS (Microgravity Advanced Research and Support) Center, Via Gianturco, 31, 80146 Napoli, Italy*
[b] *Via Salvator Rosa 53, 80046 San Giorgio a Cremano (Na), Italy*

Abstract

Secondary and oscillatory instabilities in thermal gravitational convection have been the focus of intensive studies over recent years due to their relevance in materials science, and in particular, in the field of crystal growth from the melt. The purpose of the present discussion is to provide a comparative and critical review of the subject through examination of existing studies and very recent contributions. It complements earlier reviews (Lappa, 2005) that were limited to the survey of steady three-dimensional symmetry breaking effects and/or the primary bifurcation of the flow. ***To cite this article: M. Lappa, C. R. Mecanique 335 (2007).***

Résumé

Instabilités secondaires et oscillatoires dans des modèles 3D canoniques pour la croissance cristalline. 1ère partie : des systèmes Rayleigh–Bénard. Les instabilités secondaires et oscillatoires pour la convection gravitationnelle thermique ont fait l'objet d'études intensives durant les dernières années du fait de leur pertinence en science des matériaux, et plus particulièrement dans le domaine de la croissance cristalline. Le but de la présente discussion est de fournir une revue comparative et critique du sujet par l'examen des études existantes et de contributions très récentes. Il complète les précédentes revues (Lappa, 2005) qui ont été restreintes à la brisure de symétrie tridimensionnelle dans le cas stationnaire et/ou à la première bifurcation de l'écoulement. ***Pour citer cet article : M. Lappa, C. R. Mecanique 335 (2007).***

Keywords: Computational fluid dynamic; Thermal convection; Transitions

Mots-clés : Mécanique des fluides numérique ; Transitions ; Convection thermique

1. Introduction

There has been an explosive growth in the development of new materials and processing techniques in recent years to meet the challenges posed by new applications arising in electronics, telecommunications, aerospace, and other new and traditional areas. New approaches have been developed to improve product quality, reduce cost, achieve essen-

* Correspondence to: MARS (Microgravity Advanced Research and Support) Center, Via Gianturco, 31, 80146 Napoli, Italy.
E-mail addresses: lappa@marscenter.it, marlappa@unina.it.

1631-0721/$ – see front matter
doi:10.1016/j.crme.2007.05.003

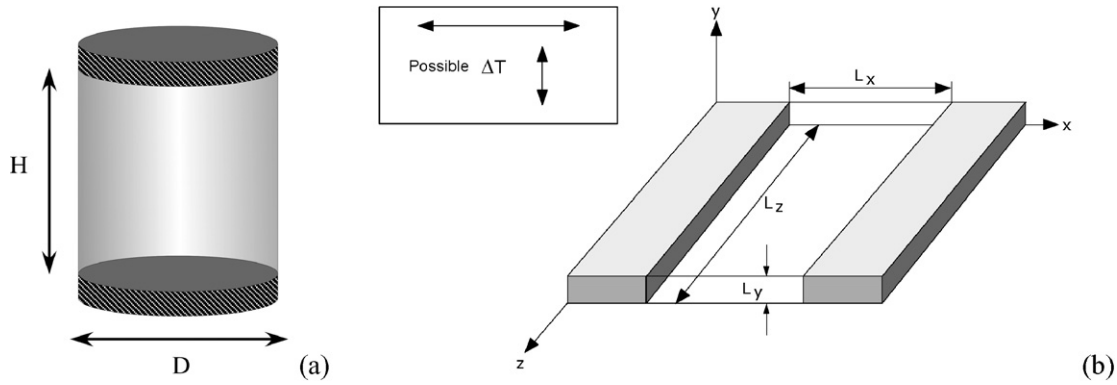

Fig. 1. Canonical geometrical models: (a) cylinder, (b) parallelepipedic enclosure.

Fig. 1. Modèles géométriques : (a) cylindrique, (b) parallélépipédique.

tially custom-made material properties and current trends indicate continued research effort in materials processing as demand for specialized materials continues to increase.

It is well known that in many circumstances the quality of the final product implicitly depends on the process of solidification. For example, during crystal growth, heat flux fluctuations from the melt to the crystal produce a cycle of crystallization and remelting at the interface. This cycle produces dislocations and other microscopic defects in the crystal (see the detailed discussion below).

For terrestrial crystal growth from a body of liquid (melt) without a magnetic field, the buoyant convection in the melt is generally oscillatory. The associated oscillations in the heat flux from the melt to the crystal produce fluctuations in the local growth rate, with alternating periods of growth and remelting in severe situations.

The elements or dopants which give the crystal the desired properties, are generally rejected during crystallization, so that there is a large dopant concentration in the melt adjacent to the growth interface. When the local growth rate decreases, dopant can diffuse away from the growth interface, leading to a lower local concentration in the crystal, and when the local growth rate increases, the crystal overtakes the rejected dopant, leading to a higher local concentration in the crystal (the spatial oscillations of the dopant concentration in the crystal are usually referred to as 'striations').

For these reasons, this article is devoted to a critical and concise analysis of thermal gravitational convection. Some effort is provided to illustrate its genesis, the governing non-dimensional parameters, the scaling properties, its structure (under various heating conditions and in different geometrical configurations, see Fig. 1) and, in particular, the stability behavior and the possible bifurcations to oscillatory regimes. Thus, the present discussion can be regarded as a necessary extension of earlier reviews (Lappa [1,2]), that were focused on primary instabilities and symmetry breaking effects.

Many existing studies are reviewed and discussed through a comparison of experimental and numerical results and theoretical arguments introduced over the years by investigators to explain the observed trends. Some up-until-now unpublished results are also used for a better presentation of some cases of interest (Figs. 2 and 3). The final goal is to clarify still unresolved controversies pertaining to the physical nature of the dominating flow instability responsible for asymmetric/oscillatory convection in various technologically important processes.

An obvious justification for the long lasting (and continuing) efforts in this field can be found, as mentioned above, in the relevance that these dynamics have in several industrial applications. However, it is rather clear that these problems have also exerted an appeal on scientists and engineers as a consequence of the complexity of the possible stages of evolution and of the nonlinear behavior. This complexity is shared with other systems in nature and constitutes a remarkable challenge for any theoretical model.

2. Relevant non-dimensional numbers

The non-dimensional numbers relevant to thermogravitational convection are the well-known Prandtl and Rayleigh numbers

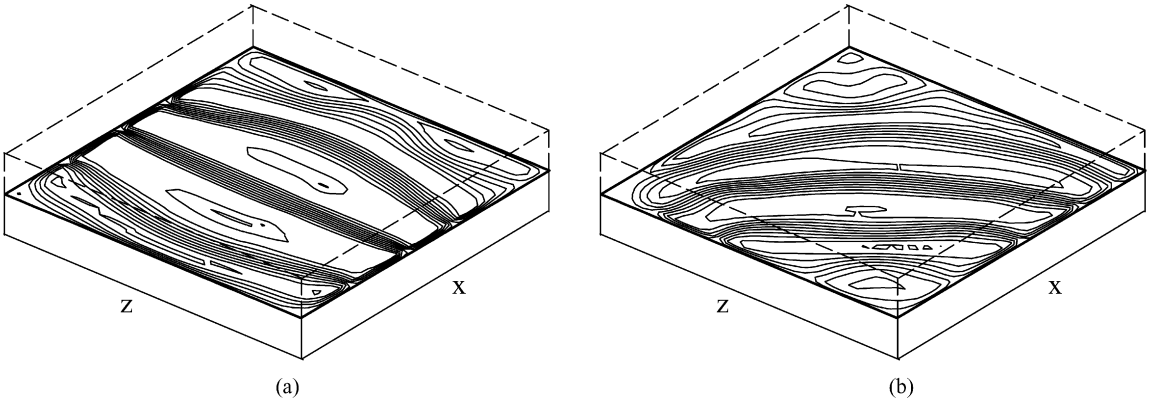

Fig. 2. Snapshots of 3D Rayleigh–Bénard convection (vertical velocity component in the horizontal midplane) in an enclosure heated from below with adiabatic lateral walls and $L_x = 4$, $L_y = 1$, $L_z = 4$ ($Pr = 0.01$, silicon, $Ra = 3 \times 10^3$, oscillatory convection) at two different times during a period of the oscillations: (a) disturbance mode with four straight rolls along the x coordinate; (b) diagonal mode with soft rolls.

Fig. 2. Convection de Rayleigh–Bénard 3D (composante verticale de la vitesse dans le plan median horizontal) dans une cavité chauffée par le bas avec des parois $L_x = 4$, $L_y = 1$, $L_z = 4$ ($Pr = 0{,}01$, silicon, $Ra = 3 \times 10^3$, convection oscillatoire) à deux differents instants d'un periode d'oscillations : (a) quatre cellules rotatives le long de la coordonnée x ; (b) mode diagonal.

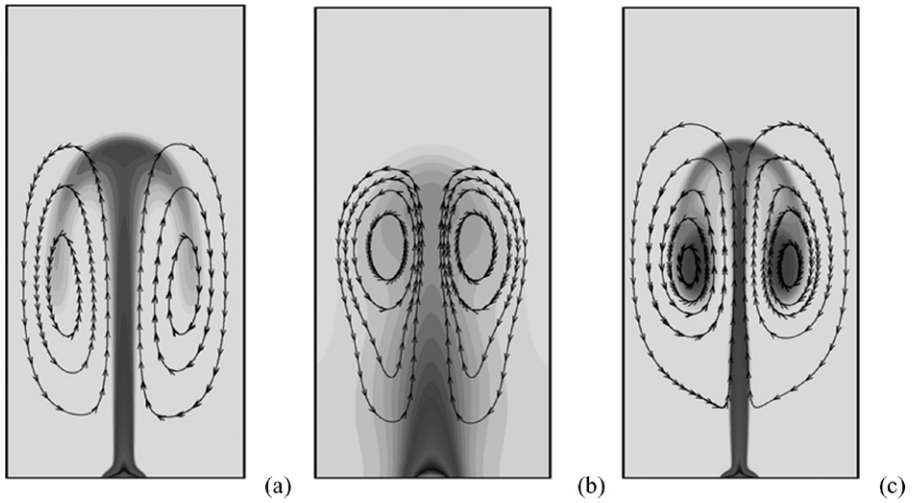

Fig. 3. Example of temperature (contour map) and velocity (streamlines) fields for various possible regimes of plume evolution (the plume is obtained by placing a line heat source at the center of the bottom surface of a box of colder fluid): (a) viscous-nondiffusive regime (VND) $Pr = 15$ and $Ra = 10^7$; (b) Inviscid-diffusive regime (IVD) $Pr = 0.01$ and $Ra = 10^7$; (c) Inviscid-nondiffusive regime (IVND) $Pr = 1$ and $Ra = 10^8$.

Fig. 3. Exemples des champs thermique (isothermes) et dynamique (lignes de courant) pour différents régimes possibles d'évolution de plumes (la plume est obtenue en plaçant une source de chaleur linéique au centre de la base d'une cavité de fluide froid) : (a) régime visqueux-nondiffusif (VND) $Pr = 15$ et $Ra = 10^7$; (b) régime non visqueux-diffusif (IVD) $Pr = 0{,}01$ et $Ra = 10^7$; (c) régime non visqueux-non diffusif (IVND) $Pr = 1$ et $Ra = 10^8$.

$$Pr = \frac{\upsilon}{\alpha} \tag{1}$$

$$Ra = \frac{g\beta_T \Delta T L^3}{\upsilon\alpha} \tag{2}$$

where υ is the kinematic viscosity, α the thermal diffusivity, g the gravity acceleration, β_T the thermal expansion coefficient, ΔT a reference temperature gradient and L a reference length for the geometrical configuration of interest.

$$Gr = Ra/Pr = \frac{g\beta_T \Delta T L^3}{\upsilon^2} \tag{3}$$

is the Grashof number which represents the ratio of buoyant to molecular viscous transport (only two of the *Gr*, *Ra* and *Pr* numbers are independent).

3. Systems heated from below: the Rayleigh–Bénard problem

For the past century, Rayleigh–Bénard convection has been the subject of very intensive theoretical, experimental and numerical studies. This problem presents, during the evolution from the stationary state to the fully developed turbulent regime, such a rich scenario of different structures and sequences of bifurcations that it is widely regarded as a reference problem for the study of different transition mechanisms in fluid dynamics.

It is known that the primary bifurcation from the quiescent condition is caused by two-dimensional perturbations of the diffusive state (see, e.g., the discussions in Gelfgat [3]) and that the threshold value of the Rayleigh number does not depend on the Prandtl number, i.e. on the model liquid used for the experiments (as shown by Luijkx and Platten [4], for rectangular containers Ra_{cr} is essentially a function of the aspect ratio). For a laterally unlimited domain, the fluid motion is regular and organized as a set of horizontal parallel rolls (quasi-two-dimensional motion, Busse [5]).

An increase of *Ra* can cause the loss of stability of these configurations, which are replaced by fully-three-dimensional flow. As shown by many authors, for the case of parallelepipedic enclosures there are several possible instability mechanisms, such as 'cross-roll', bimodal convection, and 'soft-roll', according to the Prandtl number and the wave number (the number of rolls). Under the same conditions, the Navier-Stokes equations may have more than one solution. The several solutions can be categorized according to the following classification:

(i) Quasi two-dimensional patterns in the form of rectilinear rolls consisting of (a) n transverse rolls (nT regime, n being an integer), which are orthogonal to the longest side of the parallelepipedic box (see, e.g., the experiments of Gollub and Benson [6] and Mukutmoni and Yang [7] and the numerical investigation of Stella and Bucchignani [8]); (b) n longitudinal rolls (nL regime), which are parallel to the longest side wall of the box.

(ii) Fully three-dimensional flow caused by: (a) bimodal convection, consisting of a base flow superimposed with cross rolls of approximately the same strength as the base flow (these rolls emerge at right angles to the original rolls, see, e.g., the numerical investigation of Edwards [9]); (b) distortion of the original rolls into an L shape (this configuration, called soft-roll since it is given by the superposition of two rolls whose axes are not parallel, allows a continuous transition between different wave number flow patterns, has been experimentally observed by Kolodner et al. [10] and numerically modeled by Stella et al. [11] in relatively shallow enclosures).

Within such a context it is also worth citing the recent numerical investigation (finite element method) of Tang and Tsang [12] who have found several physical phenomena, such as multicellular flow pattern, oscillatory transient solution, 'T-shaped' rolls at the ends of a rectangular box (see also Mukutmoni and Yang [13]), and roll alignment.

In these systems typically time-dependent periodic behaviors occur as a secondary bifurcation. The oscillatory instabilities of long straight parallel rolls (in shallow cavities) calculated by Clever and Busse [14] appear, e.g., as traveling waves along the rolls. The flow is characterized by a sinusoidal wave traveling the axes of the rolls, moving them alternately left and right (see also the experiments of Gollub and Benson [6]; Mukutmoni and Yang [7,15] for other possible oscillatory behaviors).

The Rayleigh number for the onset of this time-dependent flow strongly depends on the aspect ratio of the enclosure. While, as illustrated before, the first critical Rayleigh number (Ra_{cr}) depends only on the cell geometry, the critical value for the appearance of the time dependent behavior, however, is also strongly dependent on the Prandtl number (Busse [16]; Busse and Whitehead [17]). This instability occurs in low-Prandtl fluids at smaller Rayleigh than in high-Prandtl fluids. The same result was obtained by Krishnamurti [18] who investigated the time-dependent transition in a fluid layer for a wide range of Prandtl numbers ($0.025 < Pr < 8500$) and found a systematic lowering of all the critical Rayleigh numbers (except for the first, Ra_{cr}) when the Prandtl number was decreased.

The onset of oscillatory flow in three-dimensional parallelepipedic enclosures heated from below for sufficiently high values of the Rayleigh number has been recently considered (numerical simulations) by Tomita and Abe [19] and Stella and Bucchignani [8], and by Xia and Murthy [20] for different shallow and deep configurations, respectively. Bucchignani and Stella [21], in particular, have focused on the route to chaos (see also Xia and Murthy [20]).

Because of the light shed on the problem by these and earlier studies, most of the scientific community is currently aware of the importance that the control of the boundary conditions and the geometry of the container may have on the threshold values and observed flow patterns. Nonlinear effects, geometrical constraints and, in particular, the 'multiplicity of solutions' are all essential ingredients of this type of flow; the last aspect, in particular, deserves special attention. It is known, in fact, that in three-dimensional configurations several different perturbations of the basic quiescent state can become critical at close values of the Rayleigh number; this means that in a supercritical state any of these perturbations can grow possibly competing with the others.

As an example, Fig. 2, shows time-dependent convection in a shallow enclosure ($4 \times 1 \times 4$) filled with silicon melt ($Pr = 0.01$) induced for relatively small values of the Rayleigh number by 'competition' between a diagonal mode and a mode with straight rolls parallel to the sidewalls (z direction) of the shallow enclosure (the solution undergoes a continuous 'jumping' from one mode to the other).

Like the case of low parallelepipedic enclosures, a rich variety of patterns is possible in shallow cylindrical domains. Some initial studies dealing with the primary instability of the motionless thermal diffusive state are due to Charlson and Sani [22] and Buell and Catton [23]. According to these studies, the flow structure that appears after the first bifurcation from the diffusive state depends strongly on the aspect ratio and whether the lateral boundary is adiabatic or conductive.

Other authors have studied, in particular, the possible steady solutions appearing when the Rayleigh number is further increased.

Varying the Rayleigh number through different sequences of values, for a fixed aspect ratio ($A = \text{height/diameter}$) $A = 0.25$ and $Pr = 6.7$, Hof et al. [24] experimentally obtained several different stable steady patterns for the same final Rayleigh number (that they categorized in terms of their symmetry properties as "*rolls with hot fluid rising along the center*", "*rolls with cold fluid falling along the center*", "*spoke patterns with cold fluid falling along the spokes*", "*spoke patterns with hot fluid rising along the spokes*", "*axisymmetric pattern with hot fluid rising in the center*").

Similarly, Leong [25] computed several steady convective solutions (four main types of flow structure: concentric, radial, parallel and cross-rolls) for $Ra > Ra_{cr}$ (Ra based on the height of the cylinder), all of which were stable in the range $6250 \leqslant Ra \leqslant 37500$ (for aspect ratios $A = 0.125$ and $A = 0.25$ with $Pr = 7$).

In cylinders with moderate aspect ratio, the flow structure that appears after the first bifurcation from the diffusive state depends strongly on the aspect ratio and type of lateral boundary conditions. For the case of adiabatic sidewalls, in particular, the flow is axisymmetric for $A < 0.55$ ($m = 0$) and asymmetric for larger values of A ($m = 1$, where m is the number of disturbance nodes in the azimuthal direction). The transition between axisymmetric and asymmetric modes occurs around $A = 0.72$ if conductive lateral boundaries instead of adiabatic walls are considered.

In agreement with the results for other geometrical models, the thresholds for this primary (steady) instability are independent of the Prandtl number; for the adiabatic case and $0.32 < A < 0.55$, the primary bifurcation to convection occurs at $Ra_{cr} \cong 2000$ (the critical Rayleigh number behaves merely as an increasing function of the aspect ratio, e.g., $Ra_{cr} \cong 3700$ for $A = 1$ and $Ra_{cr} \cong 2250$ for $A = 0.5$, with Ra_{cr} decreasing asymptotically towards 1707 for $A \to 0$, see, e.g., Touihri et al. [26]).

The system evolution when Ra is increased beyond Ra_{cr} has been the subject of many investigations (see, e.g., Muller et al. [27], Figliola [28], Crespo Del Arco and Bontoux [29] and Neumann [30]). Some authors have clearly observed the existence of a secondary steady bifurcation. Recently, Touihri et al. [26] have investigated such possible sequence of transitions showing that for $A < 0.55$, convection sets in with the mode $m = 0$ followed by $m = 2$ and $m = 1$, whereas for $0.55 < A < 0.63$, the first mode is $m = 1$ and the next are $m = 0$ and $m = 2$, and finally for $A > 0.63$ the order of appearance is $m = 1$, $m = 2$ and $m = 0$. In such analysis the critical Rayleigh number for the secondary steady bifurcation was found to increase with the Prandtl number quadratically at low Pr and linearly at larger Pr (the considered values of the Prandtl number were 0.02, 1 and 6.7). Similar results were obtained in the earlier investigation of Crespo del Arco and Bontoux [29] who found that for $A = 2$ at low Rayleigh number the core flow exhibits characteristic features of the $m = 1$ dominant mode, whereas at elevated Rayleigh numbers secondary vortices corresponding to the $m = 0$ mode appear and develop differently in both size and magnitude according to the considered Prandtl number ($Pr = 0.02$ or 6.7 in their analysis).

Important studies also have appeared where attention was specially focused on the transition to oscillatory behaviors. In the case of very shallow cylinders the richness of possible oscillatory dynamics of the system is quite well known. For instance, the onset of 'rotating spirals' has been clearly observed in the experimental investigation for $Pr \cong 1$ and $A = \mathrm{O}(10^{-2})$ of Plapp et al. [31] and in the numerical studies of Rudiger and Feudel [32]; earlier studies,

e.g., Croquette et al. [33] and Tuckerman and Barkley [34] reported on the existence of radially propagating patterns of concentric rolls.

The nature and structure of possible oscillatory flow for $O(10^{-1}) \leqslant A \leqslant O(1)$ is still an interesting subject of investigation. Wanschura et al. [35] predicted the secondary flow to be steady except over a narrow aspect ratio range for relatively shallow cylinders ($0.32 \leqslant A \leqslant 0.34$) at $Pr = 1$, where they found oscillatory instabilities at $Ra = 25\,000$ in the form of traveling waves. More recently, Boronska and Tuckerman [36] have shown that for such parameters the bifurcation scenario guarantees that branches of standing waves and of travelling waves are created at the bifurcation, but that at most one of these branches is stable (in practice, according to nonlinear simulations the supercritical bifurcation leading to long-lived standing waves is eventually succeeded by travelling waves, both as time progresses and as the Rayleigh number is increased). Rotating and pulsating regimes (with features different with respect to those described by Boronska and Tuckerman [36] were also observed in the experiments of Hof et al. [24] in the case of $Pr = 6.7$ and $A = 0.25$.

For the case of liquid metals, in particular, complex (steady and time-dependent) supercritical regimes were simulated in cylinders of aspect ratios $A = 1$ and $A = 2$ for $Pr = 0.02$ and in ranges of Ra up to $8Ra_c$ and $6Ra_c$, respectively, by Crespo del Arco et al. [37]. Transition to fully developed turbulence for a similar configuration ($A = 1$ and $Pr = 0.022$, mercury) has been considered through three-dimensional numerical simulations by Verzicco and Camussi [38] for values of the Rayleigh number $Ra < 10^6$ and via experimental analysis by Takeshita et al. [39] for $10^6 < Ra < 10^8$ and Cioni et al. [40] for $5 \times 10^6 < Ra < 5 \times 10^9$, respectively.

Marked oscillatory phenomena have been also detected in the experiments of Kamotani et al. [41] dealing with tall cylinders ($A = 3$) and Gallium.

Within this context it is also worth citing the recent computations by Kaenton et al. [42] and Bennacer et al. [43] where the investigation of the flow instabilities has been carried out focusing on effective crystal growth configurations (Vertical Bridgman).

When the Rayleigh number is increased to relatively large values, it is known that in all these finite-size systems well-defined boundary layers develop along the solid walls and that, in general, ensuing turbulent convection is characterized by the time-dependent (often chaotic) 'release' of unsteady thermal plumes which 'detach' from the aforementioned boundary layers (see, e.g., Vincent and Yuen [44], Kadanoff [45], Qiu and Tong [46], Xi et al. [47]). In practice, there are two coherent structures, which are found to coexist in an enclosure for turbulent convection; one is the large-scale circulation (usually referred to as 'wind' or 'flywheel' that spans the height of the container, and the other is intermittent bursts of thermal plumes from the upper and lower thermal boundary layers.

The dynamics of these plumes plays a crucial role in the development of the turbulent regime and its features. For these reasons the next section is devoted to a brief survey of the properties of these plumes and of the additional instabilities which they can undergo transition to.

4. Turbulent Rayleigh–Bénard convection: plume dynamics

The theory for steady laminar plumes is well established. Scaling arguments indicate that the vertical velocity is constant (see, e.g., Batchelor [48]). Such analyses are valid for the plume stem far from the leading edge (the cap) and do not specify the cap behavior.

Recent studies about the starting (cap) behavior of thermal plumes are due to Kaminski and Jaupart [49].

It is well known since 1954, however, that as a plume rises, it widens due to the diffusion of both heat and momentum in the lateral plane (Batchelor [48]). A line source plume forms a wedge, with the angle controlled by the rate of entrainment.

Recently, Hier Majumder et al. [50], in particular, have extended these investigations to Prandtl numbers ranging from 10^{-2} up to 10^4, illustrating the possible existence of different regimes of plume growth (categorized in terms of relative thickness of thermal and velocity boundary layers along the plume body) in the Prandtl–Rayleigh space:

The *viscous-nondiffusive regime* (*VND*) is defined by thin temperature boundary layers and thick velocity boundary layers. It has thin plumes with sharp features and no strong vortices. Fig. 3(a) shows that the plume shape is clear and distinct with a thin stem. The plume has a well-defined head with side lobes. With time the plume lobes remain relatively distinct and are not significantly deformed by vortex structures. The vorticity field is featured by two broad regions of opposing vorticity on each side of the plume without sharp vortices. The thick velocity boundary layers seen in this flow result in the velocity being dissipated by viscous friction rather than by vortices.

This regime occurs at a moderate Rayleigh number ($Ra = \mathrm{O}(10^7)$) and relatively high Prandtl number ($Pr = \mathrm{O}(10)$).

The *inviscid-diffusive regime* (*IVD*) is defined by thin velocity and thick temperature boundary layers. The plume has a thick, flame-shaped stem (Fig. 3(b)). In the temperature map, it has a weakly developed head area with no lobes. The head tends to merge with the plume stem over time due to the high thermal diffusion. The head region, however, is well defined in the vorticity field by strong vortices. Vortices develop in the head region of the plume because the low viscosity does not allow viscous dissipation by diffusion.

This regime occurs at small Prandtl ($Pr = \mathrm{O}(10^{-2})$) and moderate Rayleigh numbers ($Ra = \mathrm{O}(10^6)$).

The *inviscid-nondiffusive* (*IVND*) *regime* is defined by both thin temperature and velocity boundary layers. The nondiffusive nature of the regime can be clearly observed in the temperature field. The plume has a thin, sharp stem with a well-defined cap and lobes that are significantly deformed by vortex structures.

This regime takes place for high Rayleigh numbers ($Ra > \mathrm{O}(10^6)$) and Prandtl numbers near 1.

This is the most turbulent of the possible regimes. It is characterized by fine, turbulent structures that cover a wide range of small scales. This makes the regime the most difficult one from a computational point of view. The IVND plume with $Pr = 1$ and $Ra = 10^8$ is shown in Fig. 3(c).

The plumes in all these situations are susceptible to the sinuous instabilities created by horizontal shear, which are characteristic of turbulent plumes. With time the plumes develop a sinuous, snake-like appearance due to horizontal shear. This shear can cause the plume stem to become so distorted that the local Rayleigh number becomes supercritical. This causes the original plume to collapse, and new plumes to develop from the original plume stem (see, e.g., Cortese and Balachandar [51]).

References

[1] M. Lappa, Thermal convection and related instabilities in models of crystal growth from the melt on earth and in microgravity: Past history and current status, Cryst. Res. Technol. 40 (6) (2005) 531–549.

[2] M. Lappa, On the nature and structure of possible three-dimensional steady flows in closed and open parallelepipedic and cubical containers under different heating conditions and driving forces, Fluid Dynam. Mater. Process. 1 (1) (2005) 1–19.

[3] A.Yu. Gelfgat, Different modes of Rayleigh–Bénard instability in two- and three-dimensional rectangular enclosures, J. Comput. Phys. 156 (1999) 300–324.

[4] J.M. Luijkx, J.K. Platten, On the onset of free convection in a rectangular channel, J. Non-Equilibrium Thermodynam. 6 (1981) 141.

[5] F.H. Busse, Non-stationary finite amplitude convection, J. Fluid Mech. 28 (1967) 223–239.

[6] J.P. Gollub, S.V. Benson, Many routes to turbulent convection, J. Fluid Mech. 100 (1980) 449–470.

[7] D. Mukutmoni, K.T. Yang, Rayleigh–Bénard convection in a small aspect ratio enclosure: Part I—bifurcation to oscillatory convection, ASME J. Heat Transfer 115 (1993) 360–366.

[8] F. Stella, E. Bucchignani, Rayleigh–Bénard convection in limited domains: Part 1—oscillatory flow, Numer. Heat Transfer Part A 36 (1) (1999) 1–16.

[9] D.F. Edwards, Crossed rolls at onset of convection in a rigid box, J. Fluid Mech. 191 (1988) 583–597.

[10] P. Kolodner, R. Walden, A. Passner, C. Surko, Rayleigh–Bénard convection in an intermediate aspect ratio rectangular container, J. Fluid Mech. 163 (1986) 195–226.

[11] F. Stella, G. Guj, E. Leonardi, The Rayleigh–Bénard problem in intermediate bounded domain, J. Fluid Mech. 254 (1993) 375–400.

[12] L.Q. Tang, T.T.H. Tsang, Temporal, spatial and thermal features of 3-D Rayleigh–Bénard convection by a least-squares finite element method, Comput. Methods Appl. Mech. Engrg. 140 (1997) 201–219.

[13] D. Mukutmoni, K.T. Yang, Pattern selection for Rayleigh–Bénard convection in intermediate aspect ratio boxes, Numer. Heat Transfer Part A 27 (6) (1995) 621–637.

[14] R.M. Clever, F.H. Busse, Transition to time-dependent convection, J. Fluid Mech. 65 (1974) 625–645.

[15] D. Mukutmoni, K.T. Yang, Rayleigh–Bénard convection in a small aspect ratio enclosure: Part II—bifurcation to chaos, ASME J. Heat Transfer 115 (1993) 367–376.

[16] F.H. Busse, The oscillatory instability of convection rolls in a low Prandtl number fluid, J. Fluid Mech. 52 (1972) 97–112.

[17] F.H. Busse, J.A. Whitehead, Oscillatory and collective instabilities in large Prandtl number convection, J. Fluid Mech. 66 (1974) 67–79.

[18] R. Krishnamurti, Some further studies on the transition to turbulent convection, J. Fluid Mech. 60 (1973) 285–303.

[19] H. Tomita, K. Abe, Numerical simulation of the Rayleigh–Bénard convection of air in a box of a large aspect ratio, Phys. Fluids 11 (1999) 743–745.

[20] C. Xia, J.Y. Murthy, Buoyancy-driven flow transitions in deep cavities heated from below, J. Heat Transfer 124 (4) (2002) 650–659.

[21] E. Bucchignani, F. Stella, Rayleigh–Bénard convection in limited domains: Part 2—transition to chaos, Numer. Heat Transfer Part A 36 (1) (1999) 17–34.

[22] G.S. Charlson, R. Sani, On the thermoconvective instability in a bounded cylindrical fluid layer, Int. J. Heat Mass Transfer 14 (1971) 2157–2160.

[23] J.C. Buell, I. Catton, The effect of wall conduction on the stability of a fluid in a right circular cylinder heated from below, Trans. ASME J. Heat Transfer 105 (1983) 255–260.
[24] B. Hof, G.J. Lucas, T. Mullin, Flow state multiplicity in convection, Phys. Fluids 11 (1999) 2815–2817.
[25] S.S. Leong, Numerical study of Rayleigh–Bénard convection in a cylinder, Numer. Heat Transfer Part A 41 (2002) 673–683.
[26] R. Touihri, H. Ben Hadid, D. Henry, On the onset of convective instabilities in cylindrical cavities heated from below, I. Pure thermal case. Phys. Fluids 11 (8) (1999) 2078–2088.
[27] G. Muller, G. Neumann, W. Weber, Natural convection in vertical Bridgman configurations, J. Cryst. Growth 70 (1984) 78–93.
[28] R.S. Figliola, Convection transitions within a vertical cylinder heated from below, Phys. Fluids 29 (7) (1986) 2028–2031.
[29] E. Crespo Del Arco, P. Bontoux, Numerical simulations and analysis of axisymmetric convection in a vertical cylinder: An effect of Prandtl number, Phys. Fluids A 1 (1989) 1348–1359.
[30] G. Neumann, Three-dimensional numerical simulation of buoyancy driven convection in vertical cylinders heated from below, J. Fluid Mech. 214 (1990) 559–578.
[31] B.B. Plapp, D.A. Egolf, E. Bodenschatz, W. Pesch, Dynamics and selection of giant spirals in Rayleigh–Bénard convection, Phys. Rev. Lett. 81 (1998) 5334–5337.
[32] S. Rudiger, F. Feudel, Pattern formation in Rayleigh–Bénard convection in a cylindrical container, Phys. Rev. E 62 (2000) 4927–4931.
[33] V. Croquette, M. Mory, F. Schosseler, Rayleigh–Bénard convective structures in a cylindrical container, J. Phys. 44 (1986) 293–301.
[34] L.S. Tuckerman, D. Barkley, Global bifurcation to travelling waves in axisymmetric convection, Phys. Rev. Lett. 61 (1988) 408–411.
[35] M. Wanschura, H.C. Kuhlmann, H.J. Rath, Three-dimensional instability of axisymmetric buoyant convection in cylinders heated from below, J. Fluid Mech. 326 (1996) 399–415.
[36] K. Boronska, L.S. Tuckerman, Standing and travelling waves in cylindrical Rayleigh–Bénard convection, J. Fluid Mech. 559 (2006) 279–298.
[37] E. Crespo del Arco, P. Bountoux, R.L. Sani, G. Hardin, G.P. Extrémet, Steady and oscillatory convection in vertical cylinders heated from below. Numerical simulation of asymmetric flow regimes, Adv. Space Res. 8 (12) (1988) 281–292.
[38] R. Verzicco, R. Camussi, Transitional regimes of low-Prandtl thermal convection in a cylindrical shell, Phys. Fluids 9 (5) (1997) 1287–1295.
[39] T. Takeshita, T. Segawa, J.A. Glazier, M. Sano, Thermal turbulence in mercury, Phys. Rev. Lett. 76 (1996) 1465–1468.
[40] S. Cioni, S. Ciliberto, J. Sommeria, Strongly turbulent Rayleigh–Bénard convection in mercury: comparison with results at moderate Prandtl number, J. Fluid Mech. 335 (1997) 111–140.
[41] Y. Kamotani, F.-B. Weng, S. Ostrach, J. Platt, Oscillatory natural convection of a liquid metal in circular cylinders, J. Heat Transfer 116 (1994) 627–632.
[42] J. Kaenton, E. Semma, V. Timchenko, E. Leonardi, M. El Ganaoui, G. de Vahl Davis, Effects of anisotropy and solid/liquid thermal conductivity ratio on flow instabilities during inverted Bridgman growth, Int. J. Heat Mass Transfer 47 (14–16) (2004) 3403–3413.
[43] R. Bennacer, M. El Ganaoui, E. Leonardi, Symmetry breaking of melt flow typically encountered in a Bridgman configuration heated from below, Appl. Math. Model. 30 (11) (2006) 1249–1261.
[44] A.P. Vincent, D.A. Yuen, Plumes and waves in two-dimensional turbulent thermal convection, Phys. Rev. E 60 (3) (1999) 2957–2963.
[45] L.P. Kadanoff, Turbulent heat flow: Structures and scaling, Phys. Today 54 (8) (2001) 34–39.
[46] X.-L. Qiu, P. Tong, Large-scale velocity structures in turbulent thermal convection, Phys. Rev. E 64 (3) (2001) 036304, 13 pp.
[47] H.D. Xi, S. Lam, K.Q. Xia, From laminar plumes to organized flows: the onset of large-scale circulation in turbulent thermal convection, J. Fluid Mech. 503 (2004) 47–56.
[48] G.K. Batchelor, Heat transfer by free convection across a closed cavity between vertical boundaries at different temperatures, Q. Appl. Math. 12 (1954) 209–233.
[49] E. Kaminski, C. Jaupart, Laminar starting plumes in high-Prandtl-number fluids, J. Fluid Mech. 478 (2003) 287–298.
[50] C.A. Hier Majumder, D.A. Yuen, A. Vincent, Four dynamical regimes for a starting plume model, Phys. Fluids 16 (5) (2004) 1516–1531.
[51] T. Cortese, S. Balachandar, Vortical nature of thermal plumes in turbulent convection, Phys. Fluids A 5 (1993) 3226–3232.